TiO$_2$ photocatalyst deactivation by gas-phase oxidation of heteroatom organics

José Peral [a,*], David F. Ollis [b]

[a] Departament de Química, Universitat Autònoma de Barcelona, 08193 Bellaterra, Spain
[b] Department of Chemical Engineering, North Carolina State University, Raleigh, NC 27695-7905, USA

Abstract

TiO$_2$ deactivation is studied during the gas-phase photocatalytic oxidation of organics containing three different heteroatoms: Si, N and S. Auger electron spectroscopy is used to characterize the catalyst poisoning species. A kinetic equation is presented which account for the activity vs. time observed data. Finally, an estimation is made of the equivalent monolayers of reactant converted prior total activity disappearance.

1. Introduction

Gas–solid photocatalyzed oxidation of air contaminants is currently being explored for possible application to decontamination, purification, and deodorization of the air of enclosed atmospheres (spacecraft, offices, factories, homes), or for the destruction of pollutants found in the gas streams coming from air stripping of volatile organic compounds (VOC) contaminated waters. The literature now contains examples of complete photocatalyzed ambient temperature oxidation of alkanes (methane, ethane) [1,2], alkenes (ethylene, propylene, butene) [1,3–5], aromatics (toluene [6], m-xylene [7]), trichloroethylene [8–11], aldehydes (formaldehyde, butyraldehyde) [7], and ketones (acetone [7,12]). The photocatalyzed disappearance of

prototypic odor compounds such as acetaldehyde, isobutyric acid, toluene, methylmercaptan, hydrogen sulfide, and trimethylamine, and the destruction of organics found in typical closed atmospheres have also been reported [13,14].

Catalyst lifetime is an important characteristic of commercial catalysts, yet catalyst deactivation has hardly been considered or studied in the gas–solid photocatalysis literature. The few previous studies are instructive. Cunningham and Hodnett examined oxidation of secondary alcohols [15] and found a slow deactivation. Blake and Griffin [16] examined 1-butanol oxidation; while no deactivation was reported, the slow emergence of a carboxylate peak in IR spectroscopy suggested accumulation of one or more stable species which might eventually act as inhibitors. We have reported [7] catalyst deactivation of TiO$_2$ during n-butanol oxidation with reactor fed concentration of 50–200 mg ·

* Corresponding author.

m^{-3}. This deactivation was near fully reversible by overnight treatment in pure air and continued illumination: the accumulating inhibitory material was presumably photo-oxidized, although at a slower rate than *n*-butanol itself.

Evidence for irreversible photocatalyst deactivation also exists. Where a contaminant contains an N, S, P, or Si atom, a complete oxidation might allow deposition of nitrate, sulfate, phosphate, or silicate, for example. Fox and coworkers [17] have examined photo-oxidation in liquid acetonitrile of compounds containing silicon (benzyltrimethylsilanes) and tin (benzyltrimethylstannanes); they found deactivation during oxidation of organo-Si compounds, but no noticeable activity change during oxidation of organo-Sn compounds.

The brief study of odor removal done by Suzuki et al. [13] included disappearance of molecules containing sulfur (CH_3SH, H_2S) and nitrogen (($CH_3)_3N$). No consecutive runs using the same catalyst were presented, no comment was made concerning deactivation, and no surface analysis were carried out on any used catalyst to check for deposition of oxidized material.

None of the studies mentioned above have reported rate equations for photocatalyst deactivation, nor has any quantitative relation appeared relating material deposited or presumably accumulated vs. activity loss. Also, no surface analysis of such a deactivated photocatalyst has been published.

The present work initiates examination of possible photocatalyst deactivation driven by photocatalyzed oxidation of heteroatom contaminants expected in spacecraft atmospheres, specifically decamethyltetrasiloxane (DMTS), indole, pyrrole and dimethyl sulfide (DS). Both, N and Si containing reactants produce irreversible catalyst deactivation, and Auger surface analysis confirm existence of carbon and heteroatom (N or Si) deposits on partially deactivated catalyst. In contrast, no kinetic evidence of sulfur induced deactivation is found, nor does surface analysis hint at sulfur deposition.

2. Experimental

The experimental set-up used to obtain the results presented here is similar to the one employed by Teichner and coworkers [5] and Dibble and Raupp [8], and is described in detail elsewhere [7]. An UHP air tank (Linde) was used to bring a 20.11 l gas reservoir to one atmosphere. A suitable amount of contaminant in liquid form was then injected into the reservoir through a sample port. Following complete vaporization the reservoir was filled with additional air up to a final pressure (typically $2.18 \cdot 10^5$ N · m^{-2}), which was sufficient to provide the desired gas flow rates over periods up to several hours. An air stream from the tank and a gas mixture stream from this lightly pressurized reservoir were mixed continuously, and passed to the reactor through mass flow sensor-controllers coupled to a mass flow controller unit (Linde FM4574). The photo-reactor was a cylindrical vessel (4 cm high and 3.14 cm^2 base) with an interior attached fritted glass plate used to support the powdered photocatalyst and through which the downward flow passed. An air-tight quartz window enclosed the reactor top. Two lateral ports provided the inlet and outlet for the gas mixture, and a thermocouple (always in the dark) was installed just downstream of the glass frit. The photo-excitation light source was placed directly above the reactor window. A gas sampling loop allowed capture of aliquots of either the reactant feed or the product stream. Near-UV (300–400 nm) or true-UV (254 nm) light were obtained with the same lamp (100 W UVP blacklight) by using of removing the lamp external filter. The powder catalyst was deposited by dropping 0.3 ml of a 10 g · l^{-1} suspension of TiO_2 onto the fritted glass support, allowing for room temperature evaporation of water, and finally drying the entire reactor in an oven at 120°C for 2 hours. With this procedure the TiO_2 layers obtained were reproducible and could also be recovered from the fritted glass after each run, by simply scrapping the glass surface, in order to perform

subsequent Auger Electron Spectroscopy (AES) analysis. The catalyst samples, once removed from the photo-reactor, where placed in a closed vial under N_2 atmosphere and in the dark. No pretreatment of the catalyst was carried out before the spectrophotometric measurements. A Perkin Elmer system was used for AES measurements. Gas mixtures of 200 mg · m^{-3} of the different chemicals and 1000 mg · m^{-3} of water with an air flow rate of 50 cm^3 · min^{-1} were used in all the experiments. Gas chromatography (Perkin Elmer Sigma 1) operating with a flame ionization detector and a SS Alltech column with AP-L 15% on 80/100 Chrom W packing was used for all gas chemical analyses. Because of the intrinsic limitations of the experimental system the data recollected is clearly scattered. The reactant fed concentrations have been calculated as the arithmetic mean of at least 10 consecutive GC injections. The catalyst used was P25 TiO$_2$ (Degussa) with a primary particle diameter of 30 nm, a surface area of 50 ± 15 m^2 · g^{-1}, and a crystal structure formed mainly of anatase. The P25 particles were spherical and nonporous, with a stated purity > 99.5%. Stated impurities included: Al$_2$O$_3$ (< 0.3%), HCl (< 0.3%), SiO$_2$ (< 0.2%), and Fe$_2$O$_3$ (< 0.01%). This powdered semiconductor catalyst was used as supplied without pretreatment. The DMTS, pyrrole, indole and DS used to prepare individual feed gas mixtures were of HPLC grade (Aldrich).

3. Results and discussion

3.1. DMTS photo-oxidation

Before photo-oxidation experiments, a study of the dark-adsorption of DMTS on the catalyst was carried out. Under the experimental conditions reported in the previous section, 1.69 mg of DMTS were necessary to saturate the catalyst surface, which is equivalent to a coverage of 21.8 DMTS molec · nm^{-2} of catalyst. This is a high value that indicates the importance of the

dark-adsorption phenomena of DMTS onto the catalyst. After 600–700 min of dark flow, the DMTS concentrations entering and leaving the reactor were equal, indicating that no *dark* reaction takes place.

Fig. 1a shows how DMTS effluent concentration changes with irradiation time after the achievement of a dark equilibrium and upon illumination with near UV light. An initial desorption of DMTS occurs, being the exit stream reactant concentration higher than the fed concentration (dotted line). After this initial desorption, the concentration of DMTS decreased to a minimum value of 120 mg/m^3 (44% conver-
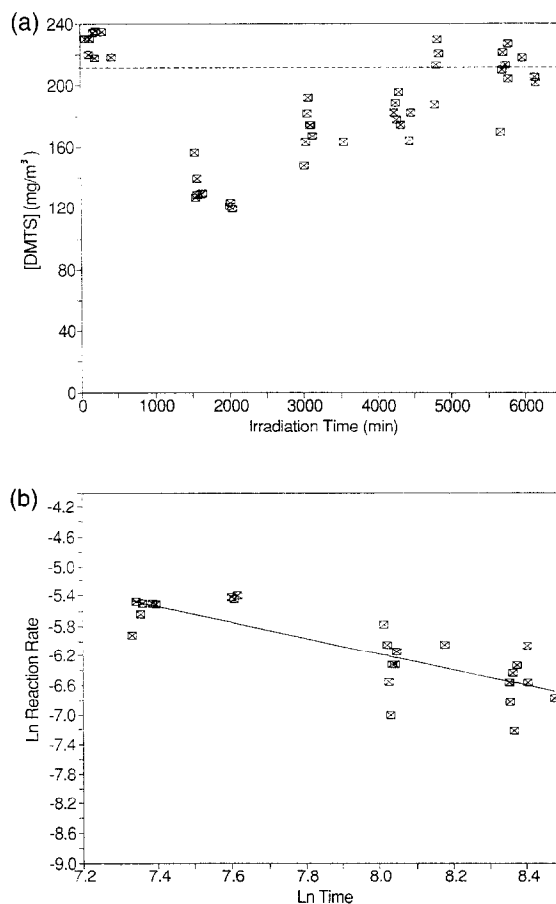

Fig. 1. Photo-catalyzed DMTS oxidation: (a) exit DMTS concentration vs. irradiation time during photo-catalyzed oxidation. The dotted line shows the reactor feed concentration of DMTS. (b) ln rate vs. ln time. [DMTS] = 200 mg · m^{-3}, [H$_2$O] = 1000 mg · m^{-3}, F = 50 cm^3 · min^{-1}.

sion). No intermediate reaction products were detected by flame ionization. As have been mentioned in the experimental section, considerable data scattering is seen, perhaps due to small temperature changes in the laboratory. Despite this inconvenience, a clear deactivation appears over the irradiation period, and after about 6000 min the photocatalytic activity completely stops. The rate of reaction in our integral conversion plug flow photo-reactor can be conveniently represented by the correlation:

$$\frac{r}{r_0} = \frac{1}{1 + t^b} \tag{1}$$

Reaction rates were calculated with the formula:

$$R = (C_0 - C)F\frac{1}{10^6} \tag{2}$$

being F the gas stream flow, C_0 and C the entering and leaving organic concentrations, and $1/10^6$ a conversion factor of m^3 to cm^3. Eq. (1) is a mathematical expression that takes into account the deactivation phenomena and is similar to other heterogeneous catalyst deactivation kinetics reported previously [18], and satisfies two experimental observations: (i) for times greater than about 1000 min, a time large enough to avoid the initial desorption phenomena, ln rate varies linearly with ln time (Fig. 1b); (ii) at $t = 0$, $r = r_0$ = initial rate of reaction. For DMTS $r_0 = 10.93$ mg · min^{-1} and $b = 1.07$ (being t expressed in min).

Taking into account the amounts of TiO_2 deposited onto the fritted glass and the DMTS reacted along the experiment and before complete TiO_2 deactivation, a ratio of conversion vs. catalyst surface available of $2 \cdot 10^{16}$ molec · cm^{-2} is calculated. If all Si atoms remained on the catalyst surface after reaction and the TiO_2 estimated surface site density is 5–$15 \cdot 10^{14}$ sites · cm^{-2}, a coverage of $8 \cdot 10^{16}$ atom · cm^{-2}, corresponding to more than one hundred monolayers of Si, would be obtained

After DMTS photo-oxidation, the AES spectrum of the TiO_2 photocatalyst (Fig. 2) con-
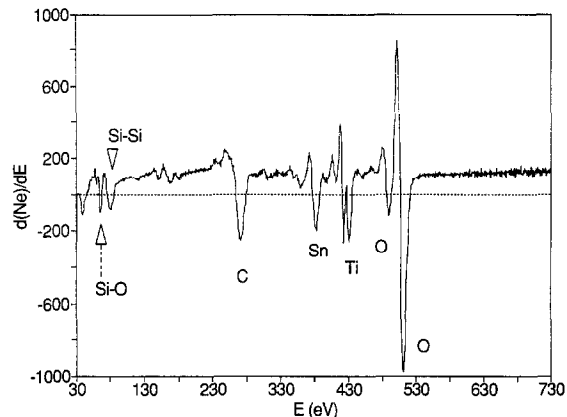

Fig. 2. Auger electron spectrum of deactivated titania photo-catalyst after DMTS photo-oxidation. The Sn peak is due to the use of an Sn metal holder for the AES analysis.

tained three important new features which were not detected in the catalysts samples used for blank runs (TiO_2 + DMTS in the dark and TiO_2 + light but no DMTS). The broad 270.8 eV peak is due to carbon deposits [19]. This detail proves that upon illumination, DMTS is not only adsorbing on the TiO_2 but is decomposing and creating carbonaceous deposits that may be responsible for a slight change in the catalyst color (white to pale yellow) noticed after illumination. The 66 eV peak is associated with Si atoms in an oxygen matrix [19]. It is unclear if SiO_2 is actually formed on the surface, as reported by others [17] in liquid-phase heterogeneous photocatalysis, or if the oxygen matrix is formed by the TiO_2 oxygen atoms bonding to isolated Si atoms. The AES peak at 81.2 eV indicated the existence of Si–Si species [19]. The presence of and Si–Si species is also evidence of DMTS decomposition reactions on the TiO_2 surface.

3.2. Pyrrole photo-oxidation

When a pyrrole–air–water vapor mixture was passed through the reactor in absence of light, no pyrrole adsorption was noticed. Fig. 3 shows how the concentration of pyrrole changed with irradiation time under different experimental conditions. When near UV light is switched on,
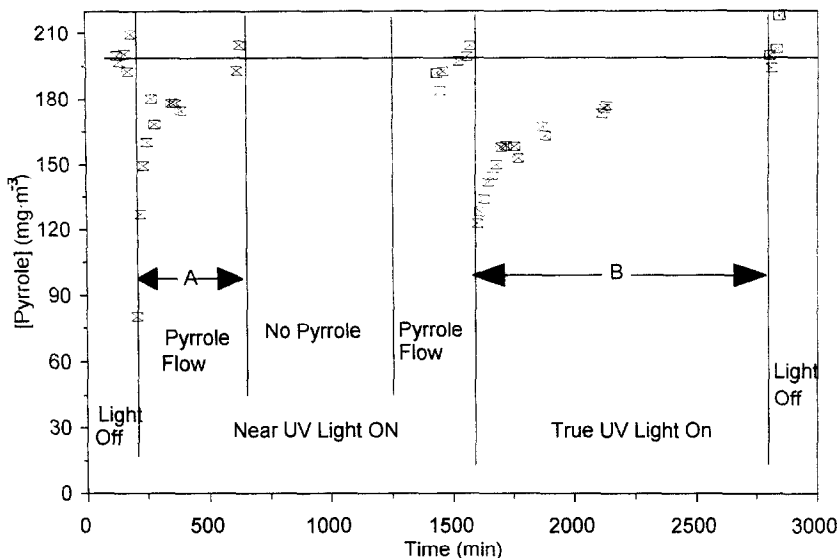
Fig. 3. Photo-catalyzed pyrrole oxidation: pyrrole concentration vs. time. Interval A: deactivaton in near UV light; interval B: deactivation in UV (254 nm) light. The dotted horizontal line indicates the pyrrole reactor feed concentration. [Pyrrole] = 200 mg · m^{-3}, [H$_2$O] = 1000 mg · m^{-3}, F = 50 cm^3 · min^{-1}.

a 60% pyrrole conversion is detected at the outlet of the reactor. This initial activity decreased continuously and completely disappeared in about 400 min. In an attempt to recover catalyst activity, the pyrrole flow was halted, and flow of a pure air–water vapor gas mixture was allowed in the reactor during 900 min of near-UV irradiation. No recovery of TiO$_2$ activity was noticed, in contrast to the regeneration found in a previous paper [7] for

1-butanol deactivated catalyst treated in the same way described here. However, when true UV light was used to illuminate the deactivated catalyst, activity is again present as shown by the clear decrease of pyrrole concentration (36% conversion); again, the activity decreases with irradiation time and completely disappears after approximately additional 1500 min. Attempts to recover the activity by overnight illumination of flowing air–water vapor mixtures were also unsuccessful.
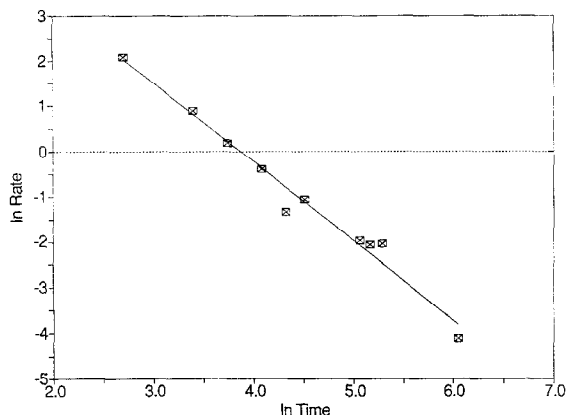

Fig. 4. Deactivation of TiO$_2$ during near-UV activated pyrrole photo-oxidation. ln reaction rate vs. ln time.
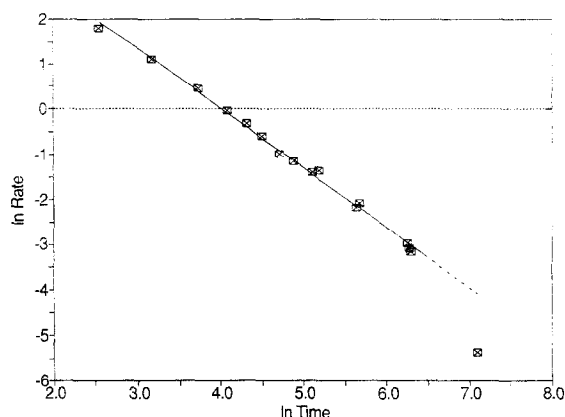

Fig. 5. Deactivation of TiO$_2$ during true-UV (254 nm) activated pyrrole photo-oxidation. ln reaction rate vs. ln time.
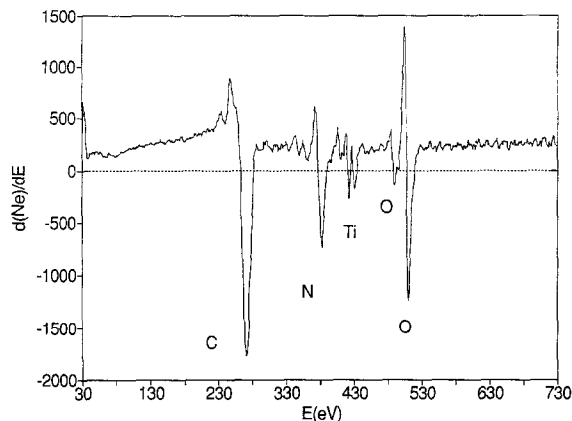
Fig. 6. Auger electron spectrum of deactivated titania photo-cata-
lyst after pyrrole photo-oxidation.

In both cases (true and near UV), the experi-
mental deactivation kinetics can be expressed as
a function of time with Eq. (1). Fig. 4 and Fig.
5 show that ln rate varies linearly with ln time,
with parameter values being $b = 1.74$ and $r_0 =$
848 mg $\cdot$ m^{-3} $\cdot$ min^{-1} for near-UV irradiation,
and $b = 1.33$ and $r_0 = 534$ mg $\cdot$ m^{-3} for UV
irradiation. It has to be emphasized that a sim-
ple exponential decay of rate vs. time does not
fit the data of either pyrrole or DMTS photo-
oxidation.

A qualitative AES analysis of the chemical
species present on the TiO$_2$ surface after pyr-
role photo-oxidation (Fig. 6) shows spectral
peaks due to deposits containing carbon (271.6
eV) and nitrogen (382.8 eV). None of these

peaks were detected in the catalysts samples
used for blank runs (TiO$_2$ + pyrrole in the dark
and TiO$_2$ + light but no pyrrole). It is important
to notice that the Ti peak (422.8 eV) is smaller
that the similar peak in Fig. 2, which means a
higher TiO$_2$ surface coverage when degrading
pyrrole. Black spots were found over the Sn foil
used as catalyst holder in the AES instrument
after recording the spectrum, probably due to
carbon deposits formed by pyrrole reduction by
the incident electron beam.

3.3. Indole photo-oxidation

Indole is a solid at room temperature, and its
equilibrium vapor pressure allowed to obtain a
gas stream concentration of 58 mg $\cdot$ m^{-3}. The
horizontal dotted line in Fig. 7 shows the indole
concentration rate obtained after saturation of
the catalyst surface in the dark. Upon irradiation
the indole concentration clearly suffers an initial
decrease, but is steadily recovered, indicating
TiO$_2$ deactivation, but at a much slower rate
than with pyrrole. The gas reservoir needed to
be replenished twice with fresh solid indole
before the catalytic activity completely disap-
peared (4600 min of irradiation). The slight
recovery of activity seen in Fig. 7 between 1800
and 2900 min is the result of the inherent
difficulty of preparing the same feed concentra-
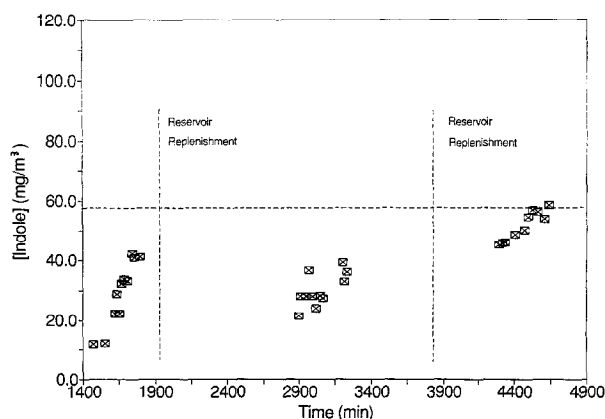tion when replenishing the reservoir. The amount

Fig. 7. Photo-catalyzed indole oxidation: indole concentration vs. irradiation time. The dotted horizontal line indicates the indole reactor
feed concentration. [Indole] = 200 mg $\cdot$ m^{-3}, [H$_2$O] = 1000 mg $\cdot$ m^{-3}, F = 50 cm^3 $\cdot$ min^{-1}.

of both nitrogen compounds, pyrrole and indole, that reacted before achieving complete catalyst deactivation was the same, $6.5 \cdot 10^{-6}$ moles, which represents $2.7 \cdot 10^{15}$ molec $\cdot$ cm^{-2}. This number represents a coverage of several mono-layers, assuming again an average concentration of Ti atoms at the surface of $\approx 5 \cdot 10^{14}$ molec/cm^2.

3.4. Dimethyl sulfide photo-oxidation

When feeding the photo-reactor with a gas mixture containing dimethyl sulfide (DS) no *dark* adsorption of this organic was observed. Upon near UV irradiation, a low steady-state conversion of 10% was obtained (Fig. 8). In this case, no deactivation was noticed during the 5000 min of irradiation that the experiment lasted. The data depicted in Fig. 8 shows only the final 1500 min of the experiment, although a previous DS photo-oxidation of 3500 min was carried out with no appreciable change in the steady-state conversion value. A dark-blue color appeared on the catalyst after approximately 100 min of illumination, but no important S signal was detected by AES measurements (Fig. 9). The very small peak at 159 eV may be associated to S (not seen in the blank runs) but even under this assumption the deposition of S on the TiO$_2$ would be very low as can be inferred from the size of the peak and the fact
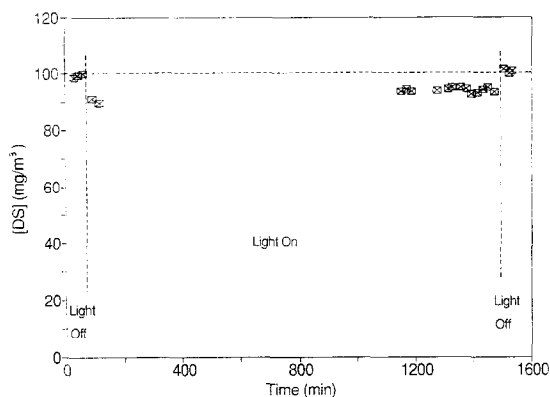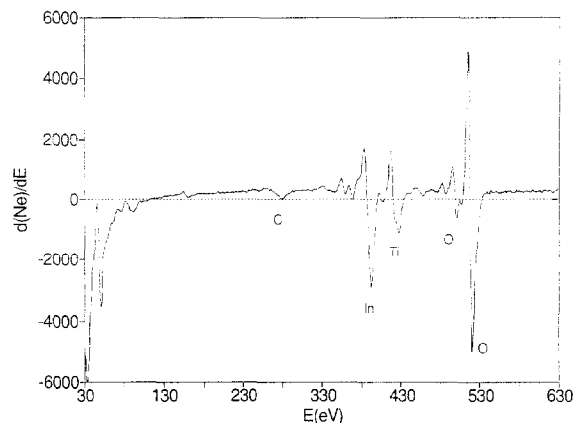

Fig. 9. Auger electron spectrum of titania photo-catalyst after DS photo-oxidation. The In peak is due to the use of an In metal holder for the AES analysis.

that S is one of the most sensitive elements for AES. Thus, no kinetic or spectroscopic evidence is obtained to indicate presence of appreciable interfering sulfate or sulfur deposition. Either S is removed continually as SO$_2$ or SO$_3$, or the mercaptan is only partly converted and the partial oxidation product still contain the S atom. The first assumption seems more likely to take place since no partial oxidation products were found by GC/FID detection.

4. Conclusions

The TiO$_2$ photocatalyzed oxidation of air contaminants containing three different het-eroatoms (Si, N and S) shows irreversible cata-lyst deactivation in the case of DMTS, pyrrole and indole, while no such a phenomena is no-ticed in the case of DS. AES surface analysis have been carried out in order to characterize the species poisoning the catalyst surface, and peaks corresponding to Si, N and carbonaceous deposits have been obtained. The irreversible and complete catalyst deactivation observed when oxidizing pyrrole and indole, both N-con-taining compounds, is produced after the con-version of several equivalent monolayers of re-actant. Si related deactivation is achieved only after the conversion of a relatively large number $\approx$ (100) of equivalent monolayers. Since these

Fig. 8. Photo-catalyzed DS oxidation: DS concentration vs. time. The dotted horizontal line indicates the DS reactor feed concentration. [DS] = 200 mg$\cdot$m^{-3}, [H$_2$O] = 1000 mg$\cdot$m^{-3}, F = 50 cm$^3\cdot$min^{-1}.

deactivations appear to be irreversible, catalyst lifetime will accordingly depend on the feed concentration of such Si- and N-containing compounds. In an integral conversion, plug flow photo-reactor, destruction rate is more easily correlated as ln rate vs. ln time than as ln rate vs. time.

Acknowledgements

References

[1] S.J. Teichner and M. Formenti, in: Photoelectrochemistry, Photocatalysis and Photoreactors, ed. M. Schiavello (Reidel, New York, 1985) pp. 457–489.

[2] M. Grätzel, K. Ravindranathan and J. Kiwi, J. Phys. Chem. 93 (1989) 4128.

[3] P.C. Gravelle, F. Juillet, P. Meriaudeau and S.J. Teichner, Discuss. Faraday Soc. 52 (1971) 140.

[4] M. Formenti, F. Juillet, P. Meriaudeau and S.J. Teichner, Chem. Technol. 1 (1971) 680.

[5] H. Courbon, M. Formenti, F. Juillet, A. Lisachenko, J. Martin and S.J. Teichner, Kinet. Catal. 14 (1973) 84.

[6] T. Ibusuki and K. Takeuchi, Atmos. Environ. 20 (1986) 1711.

[7] J. Peral and D.F. Ollis, J. Catal. 136 (1992) 554.

[8] L.A. Dibble and G.B. Raupp, Catal. Lett. 4 (1990) 345.

[9] M.R. Nimlos, W.A. Jacoby, D.M. Blake and T.A. Milne, Environ. Sci. Technol. 27 (1993) 95.

[10] W.A. Jacoby, M.R. Nimlos, D.M. Blake, R.D. Noble and C.A. Koval, 28 (1994) 1661.

[11] S. Yamazaki-Nishida, K.S. Nagano, L.A. Phillips, S. Cervera-March and M.A. Anderson J. Photochem. Photobiol. A: Chem. 70 (1993) 95.

[12] R.I. Bickley, G. Munuera and F.S. Stone, J. Catal. 31 (1973) 398.

[13] K. Suzuki, S. Satoh and T. Yoshida, Oenki Kagaku 59 (1991) 521.

[14] T.N. Obee and R.T. Brown, Environ. Sci. Technol. 29 (1995) 1223.

[15] J. Cunningham and B.K. Hodnett, J. Chem. Soc., Faraday Trans. 1, 77 (1981) 2777.

[16] N.R. Blake and G.L. Griffin, J. Phys. Chem. 92 (1988) 5698.

[17] M.T. Dulay, D. Washington-Dedeaux and M.A. Fox, J. Photochem. Photobiol. A: Chem. 61 (1991) 153.

[18] H.S. Fogler, Elements of Chemical Reaction Engineering (Prentice-Hall, New York, 1986) pp. 273–274.

[19] L.E. Davis, Handbook of Auger Electron Spectroscopy, Physical Electronic Industries, Inc. (1976).